24

Feasibility Study on an Excavation-Type Demining Robot "PEACE"

Yoshikazu Mori
Ibaraki University
Japan

1. Introduction

It is said that 60 - 70 million mines are currently laid in over 50 countries throughout the world (Shimoi, 2002). These mines not only injure people directly, but also negatively influence the lives of inhabitants and restoration of the economy because of their consequent restriction of farmland. Such mines are categorized into two types: ATMs (anti-tank mines) and APMs (anti-personnel mines). The purpose of ATMs is to destroy tanks and vehicles, while that of the APMs is to injure or kill people. The APMs are cheap to produce, while APM removal is quite expensive. Also, the APMs maintain their destructive power for a long time. To mitigate the current tragic situation, an urgent "humanitarian demining operation" (with a demining rate of more than 99.7%) is now required all over the world (Shimoi, 2002).

The demining work mainly depends on hazardous manual removal by humans; it presents serious safety and efficiency issues. For increased safety and efficiency, some large-sized machines have been developed. For example, the German *MgM Rotar* rotates a cylindrical cage attached in front of the body and separates mines from soil (Geneva International Centre for Humanitarian Demining, 2002; Shibata, 2001). The *RHINO Earth Tiller*, also made in Germany, has a large-sized rotor in front of the body; it crushes mines while tilling soil (see Fig. 1). The advantages of *MgM Rotar* and *RHINO* are a high clearance capability (99%) and high efficiency respectively.

In Japan, Yamanashi Hitachi Construction Machinery Co., Ltd. has developed a demining machine based on a hydraulic shovel. A rotary cutter attached to the end of the arm destroys mines; the cutter is also used for cutting grasses and bushes. Although many machines with various techniques have been developed, a comprehensive solution that is superior to human manual removal remains elusive. Salient problems are the demining rate, limitation of demining area (*MgM Rotar*), prohibitive weight and limitation of mine type (*RHINO Earth Tiller*), and demining efficiency (*MgM Rotar, and the demining machine made by Yamanashi Hitachi Construction Machinery Co., Ltd.*). Because those machines are operated manually or by remote control, expert operators are required for each machine. Also, working hours are limited.

Recently, various demining robots have been developing mainly at universities. Hirose *et al*. have developed a probe-type mine detecting sensor that replaces a conventional prod (Kama et al., 2000). It increases safety and reliability. They have also developed a quadruped walking robot, some snake-type robots, mechanical master-slave hands to remove landmines, and robotic system with pantograph manipulator (Hirose et al., 2001a;

Hirose et al., 2001b; Furihata et al., 2004; Tojo et al., 2004). Nonami *et al*. have developed a locomotion robot with six legs for mine detection (Shiraishi et al., 2002). A highly sensitive metal detector installed on the bottom of each foot detects mines and marks the ground. Ushijima *et al*. proposes a mine detecting system using an airship (Ushijima, 2001). On this system, the airship has a control system and a detecting system for mines using electromagnetic waves; it flies over the minefield autonomously. These studies mainly address mine detection; it is difficult to infer that they effectively consider all processes from detection to disposal.
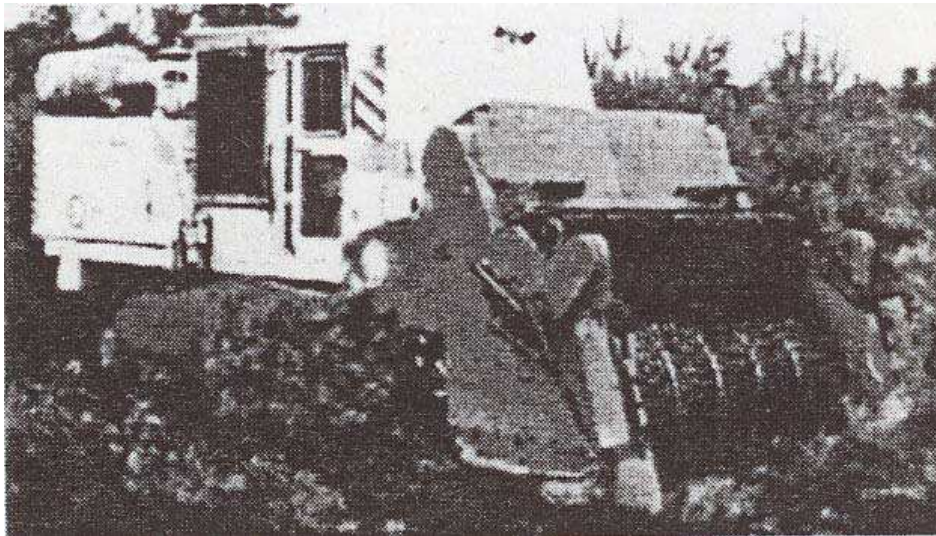

Fig. 1. Mine removal machine (RHINO Earth Tiller).

This study proposes an excavation-type demining robot "PEACE" for farmland aiming at "complete removal" and "automation"; it also presents the possibility of its realization. The robot has a large bucket in front of the body and can travel while maintaining a target depth by tilting the bucket. The robot takes soil into the body and crushes the soil, which includes mines. It then removes broken mine fragments and restores the soil, previously polluted by mines, to a clean condition. In the process, the soil is cultivated, so the land is available for farm use immediately. Expert robot operators are not required; the robot works all day long because it can be controlled autonomously.

Section 2 presents the conceptual design of the excavation-type demining robot "PEACE". Section 3 describes robot kinematics and trajectory planning. In Section 4, the optimal depth of the excavation is discussed. Section 5 shows experimental results of traveling with digging soil by a scale model of the robot. In Section 6, the structure of the crusher and parameters for crush process are discussed through several experiments. Finally, Section 7 contains summary and future works.

2. Conceptual Design of PEACE

We propose an excavation-type demining robot for farmland aiming at "complete removal" and "automation"(Mori et al., 2003, Mori et al., 2005). The reason why we

choose farmland as the demining area is as follows: farmland is such an area where local people cannot help entering to live, so it should be given the highest priority (Jimbo, 1997). Needless to say, the first keyword "complete removal" is inevitable and is the most important. The second one "automation" has two meanings, that is, safety and efficiency. In the conventional research, detection and removal of mines are considered as different works, and the removal is after the detection. However, in the case of the excavation-type demining robot, detecting work will be omitted because the robot disposes of all mines in the target area. As the result, no error caused in the detecting work brings the demining rate near to 100%.

The conceptual design of the robot is shown in Fig. 2. The robot uses crawlers for the transfer mechanism because of their high ground-adaptability. The robot has a large bucket on its front. A mine crusher is inside the bucket, and a metal separator is in its body. The first process of demining is to take soil into the body using the bucket. Figure 3 shows the excavating force on the contact point between the bucket and ground. Torque T is generated at the base of the bucket when the bucket rotates. The torque T generates force F_t against the ground. The body generates propelling force F_v. As the result, contact force F is generated as the resultant force. The rotational direction of the bucket decides the direction of the contact force F. Therefore, the robot can realize both upward motion and downward motion by adjusting the bucket torque T and the propelling force F_v. Furthermore, the robot can advance while maintaining a target depth by using some sensors.

The next process is to crush mines. The soil is conveyed into the bucket by the conveyor belt 1 in Fig. 2. As the soil is immediately carried, the strong propelling force of the body is not required. The soil, which includes mines, is crushed by the crusher. Most of the blast with the crush escapes from the lattice 4 because the fore of the bucket is underground when demining. The crusher and the bucket are hardly damaged because the explosive power of APMs is so weak to the metal. The sufficient thickness of the steel plate is about 1 cm (Geneva International Centre for Humanitarian Demining, 2002).

The last process is to separate metal splinters of mines from the soil using a metal separator. Crushed debris are conveyed by the conveyer belt 2 in Fig. 2. The metal splinters, which are used for recycling, can be selected by an electromagnet. The rest are discharged from the rear.

1. Conveyor belt 1   2. Sensors for ATM
3. Crusher   4. Lattice
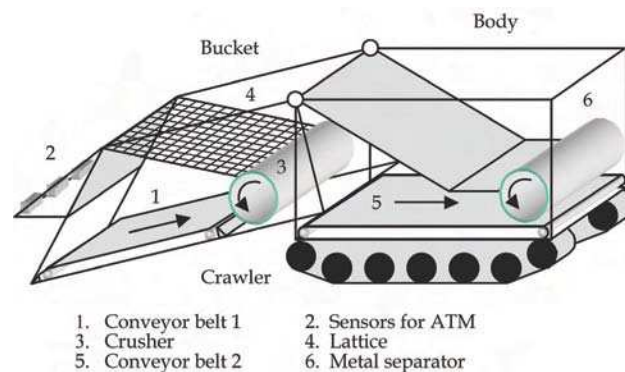5. Conveyor belt 2   6. Metal separator

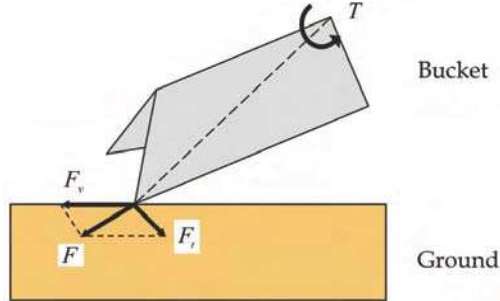Fig. 2. Conceptual design of the robot.

Fig. 3. Excavating force on the contact point.

The merits and some supplementary explanations of this mechanism are as follows:

1. This mechanism can cope with all types of mines irrespective of the size, form, and material of the mine.
2. After a series of processes, the area is available for farm use immediately as the soil becomes clean and tilled.
3. If the size of the lattice 4 is proper, uncrushed mines cannot go outside through the lattice. The uncrushed mines escaped from the bucket will be few because the clearance between the bucket and the ground is narrow and the blast will brow through the lattice. The mines will not scatter in the distance, and they will be taken into the bucket again in a short time.
4. The number of ATMs (anti-tank mines) is much smaller than that of APMs (anti-personnel mines). It is relatively easy to search for ATMs because they are larger and include more metal parts than APMs. In addition, ATMs are easy to handle because they are difficult to ignite. ATMs are detected in advance of being taken into the bucket by the several sensors: metal detectors or ground penetrating radars attached in front of the bucket. If the robot detects ATMs, it stops before them, and the work is restarted after disposing the ATMs with another method. We are now considering the details of the treatment.

3. Kinematics and Trajectory Planning

The coordinate system of the robot is shown in Fig. 4. The origins of the coordinate system Σ_{b1} and Σ_{m2} are the same.

Σ_f : Coordinate system relative to the ground,

Σ_b : Coordinate system relative to the body,

Σ_{bi} : Coordinate systems relative to each corner of the body,

Σ_m : Coordinate system relative to the bucket,

Σ_{mi} : Coordinate systems relative to each corner of the bucket,

for $i = 1,2,\cdots,4$.

Each variable and constant are as follows:

$^{*1}P_{*2} = (^{*1}x_{*2}, {}^{*1}y_{*2}, {}^{*1}z_{*2})$: Vector from the origin in coordinate system Σ_{*1} to that in coordinate system Σ_{*2} .

$^{*1}\theta_{*2}$: Angle from the x-axis in coordinate system Σ_{*1} to that in coordinate system Σ_{*2} .

$^{*1}L_{*2}^{*3}$: Constant length from the origin in coordinate system Σ_{*1} to that in coordinate system Σ_{*2} . The length is the value of *3 -axis, that is x or z , in coordinate system Σ_{*1} .

The following coordinates are derived by calculating the homogeneous transform from coordinate system Σ_f to coordinate system Σ_{m4} .

$$^f x_{m4} = {}^{m2}L_{m4}^x \cos(^f\theta_b + {}^{b1}\theta_{m2}) - {}^{m2}L_{m4}^z \sin(^f\theta_b + {}^{b1}\theta_{m2}) + {}^bL_{b1}^x \cos {}^f\theta_b - {}^bL_{b1}^z \sin {}^f\theta_b + {}^f x_b , \tag{1}$$

$$^f z_{m4} = {}^{m2}L_{m4}^x \sin(^f\theta_b + {}^{b1}\theta_{m2}) + {}^{m2}L_{m4}^z \cos(^f\theta_b + {}^{b1}\theta_{m2}) + {}^bL_{b1}^x \sin {}^f\theta_b + {}^bL_{b1}^z \cos {}^f\theta_b + {}^f z_b . \tag{2}$$

From eq. (2), the control angle of the bucket $^{b1}\theta_{m2}$ is derived as eq. (3), where the height of the robot $^f z_b$ can be measured by using some sensors like GPS and the inclinational angle of the body $^f\theta_b$ can be measured by using a clinometer. Therefore, the target angle of $^{b1}\theta_{m2}$ can be calculated if the height of the end of the bucket $^f z_{m4}$ is given as the target value. For example, at the beginning of digging, the sign of $^f z_{m4}$ is minus, and it is constant when the robot advances while maintaining a target depth. The body position $^f x_b$ can be derived as eq. (4) by substituting $^{b1}\theta_{m2}$ in eq. (3) for eq. (1). The traveling body velocity $^f\dot{x}_b$ is the derivation in time of eq. (4) and the velocity can be calculated if the bucket velocity $^f\dot{x}_{m4}$ is given as the target value.
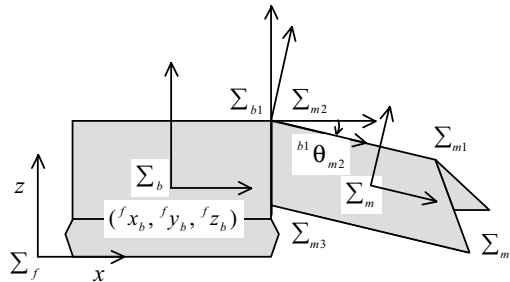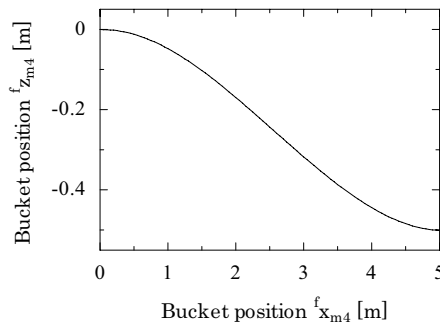

Fig. 4. Coordinate system and parameters.
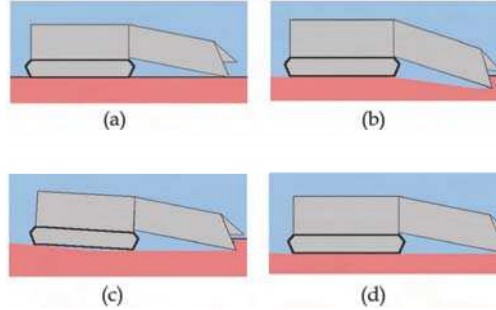

Fig. 5. Trajectory of the bucket position.

Fig. 6. Sequence of the excavation motion.

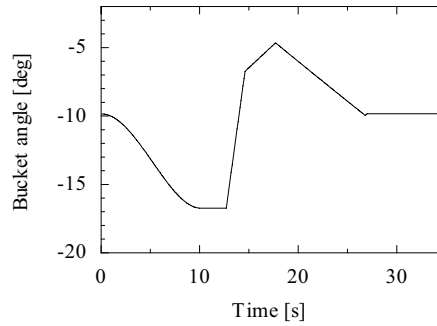Fig. 7. Simulation of the excavation motion.

$$^{b1}\theta_{m2} = \sin^{-1}\left\{\frac{^{f}z_{m4} - {}^{b}L_{b1}^{x}\sin{}^{f}\theta_{b} - {}^{b}L_{b1}^{z}\cos{}^{f}\theta_{b} - {}^{f}z_{b}}{\sqrt{\left({}^{m2}L_{m4}^{x}\right)^{2} + \left({}^{m2}L_{m4}^{z}\right)^{2}}}\right\} - \tan^{-1}\frac{{}^{m2}L_{m4}^{z}}{{}^{m2}L_{m4}^{x}} - {}^{f}\theta_{b}' \tag{3}$$

$$^{f}x_{b} = -{}^{m2}L_{m4}^{x}\cos({}^{f}\theta_{b} + {}^{b1}\theta_{m2}) + {}^{m2}L_{m4}^{z}\sin({}^{f}\theta_{b} + {}^{b1}\theta_{m2}) - {}^{b}L_{b1}^{x}\cos{}^{f}\theta_{b} + {}^{b}L_{b1}^{z}\sin{}^{f}\theta_{b} + {}^{f}x_{m4}. \tag{4}$$

Next, the trajectory of the bucket is discussed. The robot starts to dig by lowering its bucket while proceeding, and it descends the slope that is made by the bucket. The target shape of the slope based on a cubic polynomial is shown in Fig. 5. That is the trajectory of the end of the bucket. The target depth was 50 cm and the slope was generated for 20 s, and then it went ahead while maintaining a target depth. The simulation result of the whole process is shown in Fig. 6, and the time response of the bucket angle $^{b1}\theta_{m2}$ is shown in Fig. 7. The bucket angle does not change smoothly after about 12 s because the body tilts while it descends the slope.

4. Optimal Depth of Excavation

Generally, APMs are laid on the surface of the ground from 1 cm to 2 cm in depth (Shimoi, 2002). However, it is possible that they are buried in the ground by deposits. It is true that deep excavation leads to safety, but the depth beyond necessity is not realistic from the aspect of working hours and cost. In this section, we discuss which depth is appropriate.

We assumed the following: The ground is an elastic plate of the semi-infinite. Uniformly distributed load q is taken on a rectangular plate that is put on the surface of the ground.

Then normal stress to vertical direction σ_z, which passes through the center of the plate, is calculated using the theoretical formula of *Fröhlich*,

$$\sigma_z = \frac{Vqz^V}{2\pi} \int_{x=\frac{-L}{2}}^{\frac{L}{2}} \int_{y=\frac{-B}{2}}^{\frac{B}{2}} (x^2 + y^2 + z^2)^{-\frac{V}{2}-1} dxdy \tag{5}$$

where V is the stress concentration factor, z is the depth from the surface of the ground, L and B are the length and width of the rectangular plate respectively. The value of V depends on the elastic property of the soil, and it is appropriate that $V = 3$ is for clay soil and $V = 4$-5 is for sand deposit.

In this study, we examined the earth load in the ground to verify eq. (5). At first, standard sand, of which particle size was about 0.2 mm, was put into a poly container by 20 cm in depth. The capacity of the container was 300 l, and the diameter and the height were 87 cm and 70.5 cm respectively. Then the earth pressure gauge was put on the center of the surface of the soil. The maximum load of the gauge was 2 kgf/cm². Next, some soil was deposited on it and was hardened softly and evenly, and then the earth load was measured when a test subject put weight quietly on the rectangular plate in his one foot. The test subject was a man whose weight was 60 kg. The rectangular plate was wooden, and the size was 9 cm×22.6 cm and the thickness was 1.2 cm. The area of the plate was based on that of the shoe of 26 cm. We measured the earth load each five times about 10 cm, 20 cm, 30 cm, 40 cm and 47.7 cm in depth, and regarded each average as the representative value.

The result was shown in Fig. 8. The closed circle in Fig. 8 represents the earth load without additional weight, while the open circle represents the earth load when the test subject put weight on the surface. The dashed line was based on the least squares approximation of the earth load without additional weight, while the continuous line was calculated by the theoretical formula of *Fröhlich* eq. (5) when V equals 5. The dotted line represents the ignition pressure of PMN, Type72, MD82B and PMN2, which are the representative APMs.

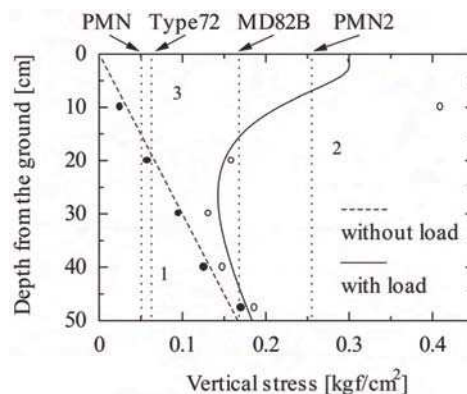

Fig. 8. Soil pressure (V =5).

In Fig. 8, for example, a straight line that passes through the point of 30 cm in depth crosses with a line and a curve at about 0.1 and 0.15 kgf/cm² respectively. In this case, the pressure only of the soil is 0.1 kgf/cm², and it changes to 0.15 kgf/cm² when the test subject puts weight on the surface. The mines of which ignition pressure is less than 0.1 kgf/cm² hardly remain unexploded because almost all of them explode under the earth

load. The mine of which ignition pressure is from 0.1 kgf/cm^2 to 0.15 kgf/cm^2 explodes when the test subject puts on it. The mine of which ignition pressure is more than 0.15 kgf/cm^2, however, does not explode with the test subject who weighs 60 kg because the ignition pressure is over the total load of the soil and him. Summarizing the above, there are few mines in the area of 1. Mines are not active in the area of 2. Mines will explode if the test subject steps into the area of 3. It is desirable that the area between 1 and 2 is narrow. However, deep excavation results in high cost. In addition, a certain amount of overburden will contribute to preventing the immense damage. Figure 9 shows the result to various stress concentration factors V. In case of sand: $V = 5$ or in case of Fig. 8, vertical stress σ_z was highest on a certain depth. That means the environment of sand is the most dangerous because the area of 3 in Fig. 8 is widest. Therefore, it was confirmed that 40 cm was proper depth.

Next, we discuss the dynamic load. The continuous line in Fig. 10 shows the experimental results when the test subject walked on the surface of the soil. The depths of the soil were from 10 cm to 40 cm. The dashed lines show the experimental results for the static loads. From this result, we can see that the load on the surface did not influence the underground so much when the depth was over 30 cm.
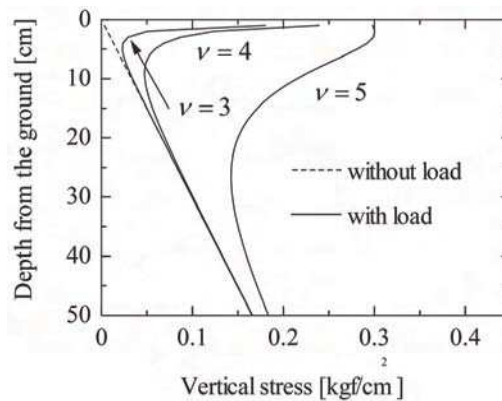
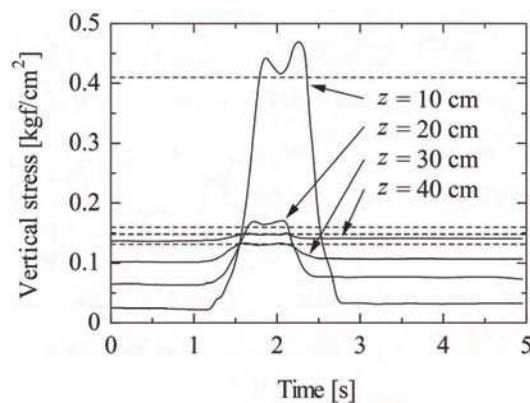Fig. 9. Relationship between the vertical stress and V.

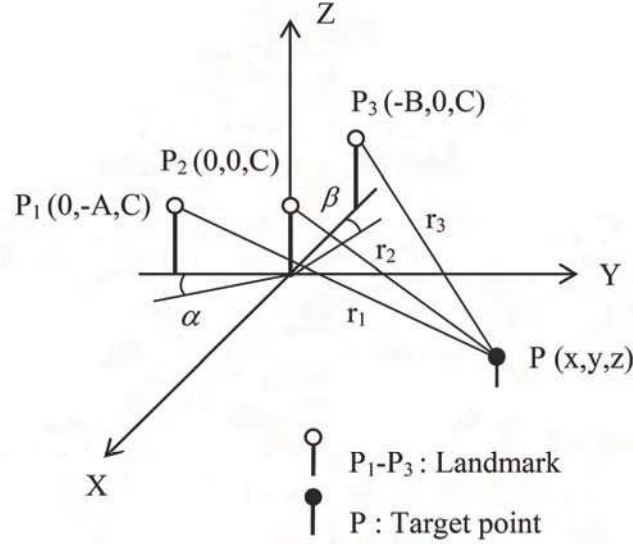Fig. 10. Time response of the soil pressure when walking.

Fig. 11. Position identification.

In conclusion, we propose 40 cm as the best excavation depth. This depth is also valid for farmland. In case mines are buried in a leaning position or that the soil has solidified with passing years, the mines become difficult to explode. Therefore, the proposed excavation depth is safer.

5. Hardware of the Scale Model

In order to control the robot autonomously, it is necessary to measure the position of the robot ($^f x_b$, $^f y_b$, $^f z_b$). In the actual robot, it will be measured by using GPS. High-precision GPS (RTK-GPS) is, however, expensive and difficult to use indoors, so a high-precision and inexpensive positioning sensor was produced in this study.

The positioning sensor is a landmark system. Three landmarks P_1, P_2, P_3 are set above the y-axis (0, $-A$, C), origin (0,0,C), x-axis ($-B$, 0, C) respectively as Fig. 11, and the heights of them are the same. Each distance from the robot is r_i (i =1,2,3). The angles α and β are the angular errors that are caused when installing the positioning sensor units. The position of the robot P (x,y ,z) is derived as follows:

$$\begin{bmatrix} x \\ y \end{bmatrix} = \frac{1}{\eta} \begin{bmatrix} \sin\beta & \cos\alpha \\ \cos\beta & \sin\alpha \end{bmatrix} \begin{bmatrix} B\,(r_1^2 - r_2^2 - A^2) \\ A\,(r_3^2 - r_2^2 - B^2) \end{bmatrix},$$ (6)

$$z = C - \sqrt{r_2^2 - x^2 - y^2}$$ (7)

where

$$\eta = 2AB\cos(\alpha + \beta)$$ (8)

The sign before the root in eq. (7) is negative if the landmark is above the robot.
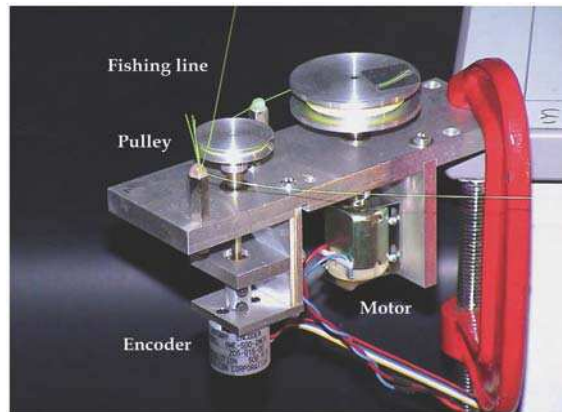
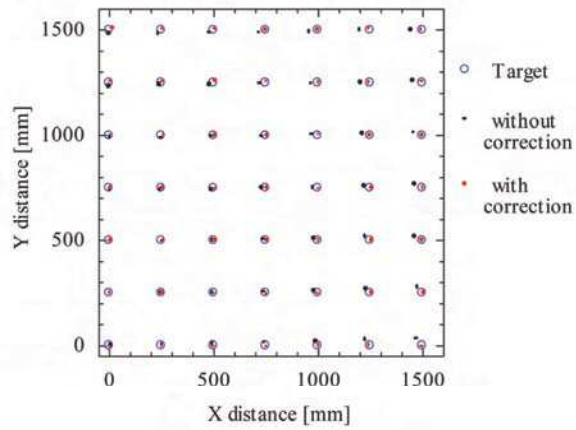Fig. 12. Positioning sensor unit.

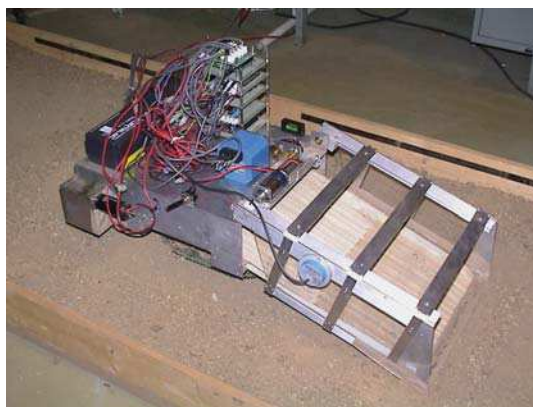

Fig. 13. Result of the position measurement.

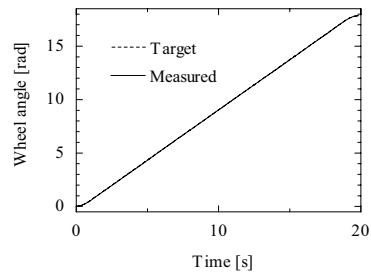Fig. 14. Excavation type mine removal robot.
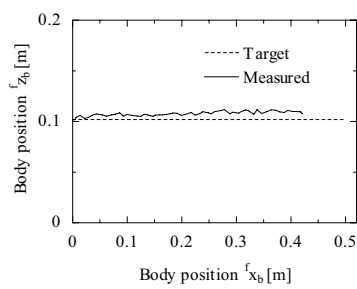
Fig. 15. Time response of the wheel angle.
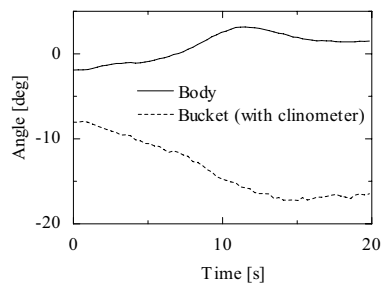

Fig. 16. Body position.

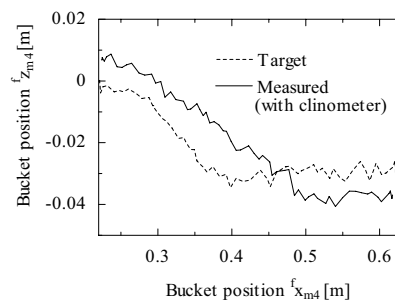Fig. 17. Time response of the body angle and bucket angle.

Fig. 18. Time response of the bucket position.

Figure 12 shows a photograph of one positioning sensor unit. A fishing line is wound round a pulley connected to an encoder. The line is stretched tight because a fixed voltage is applied on a motor that winds the line. It is possible to measure the position P (x, y, z) by using three sensor units in theory. In that case, however, it was clarified that large errors on z-axis occurred through experiments. The measure for that is to attach one more sensor unit on z-axis.

To estimate the accuracy of the positioning sensor on the x-y plane, positions of lattice points in the area of 1.5 m square were measured in every 0.25 m. The result is shown in Fig. 13. The maximum error was approximately 5.56 cm. After corrections about α, β and the diameter of the pulley connected to each encoder, the maximum error was approximately 0.69 cm.

The model of the excavation-type demining robot has a scale of 1 to 10. The dimensions of the robot are 0.36 m × 0.84 m × 0.217 m in height. The photograph is shown in Fig. 14. The crawlers for the transfer mechanism are the parts of a model tank. Each crawler can be rotated independently by a motor with an encoder. The inclinational angle of the body was measured by a fiber optical gyroscope (JG-108FD1, Resolution < 0.01 deg, Frequency response 20 Hz; Japan Aviation Electronics Industry, Ltd.). The bucket angle was measured by a clinometer (NG3, Resolution < 0.003 deg, Frequency response > 3.3 Hz; SEIKA Mikrosystemtechnik GmbH) and a potentiometer; the former was used for monitoring the bucket angle and the latter was for control. The soil in the bucket was carried by a conveyor belt to the body and discharged backward of the body without being crushed. The robot was controlled by a PD controller.

Figures 15-18 show the experimental results. The robot went through 50 cm distance in 20 s. The bucket reached the target depth of 3 cm in 10 s and kept it afterward. The measured data of the wheel angle almost agreed with the target. Figure 15 shows the time response of the wheel angle. Figure 16 shows the position of the robot ($^f x_b$, $^f z_b$) that was measured by using three positioning sensor units shown in Fig. 12 installed with tilting 90 deg. The errors were mainly caused by the unevenness of the ground and the slippage of the crawler. Those errors can be reduced if the measured position of the robot is programmed in the feedback control loop. Figure 17 shows the time response of the bucket angle measured with the clinometer and the inclinational angle of the body. The body was lifted slightly by the drag from the bucket. Figure 18 shows the bucket position ($^f x_{m4}$, $^f z_{m4}$) that was calculated from eqs. (1) and (2) based on the bucket angle measured with the clinometer. The shape of it resembled Fig. 5. The vibration of the target trajectory was caused by the measured position and inclinational angle of the body. The bucket followed the trajectory and dug to near the goal depth.

6. Crush Process

The processing reliability of demining machines or robots is the most important to humanitarian demining. The main point is the crush process. Most conventional rotor-type demining machines have rotor bits that are larger than mines. Therefore, it is possible that the mines do not touch the bits and they are left unprocessed. In addition, high reliability cannot be realized without the sifting process. Almost all of conventional machines, however, have no such process. Although MgM Rotar has this process, the demining efficiency is not so high (Geneva International Centre for Humanitarian Demining, 2002). We discuss the structure of the crusher. We made the test

equipment shown in Figs. 19 and 20 in order to examine the validity of it and the improved points. The characteristics are as follows:

1. The rotational frequency of the rotor is rapid so that the debris may become small.
2. Small rotor bits are mounted around the rotor in small intervals, and every line is mutually different.
3. The plate shown in Fig. 19 is installed under the rotor of which direction of rotation is anticlockwise.

Because of the characteristics 2 and 3, sifting process is realized.

The width of the test equipment was 554 mm, the length was 450 mm, and the height was 280 mm. The diameter of the rotor was 100 mm without bits, and its width was 207 mm. Setscrews of M5 were used for the bits. Each lateral interval of bits was 10 mm, and twenty-four bits were mounted around the circumference of the rotor. The rotor was driven by DC motor of 250 W, and its rotational frequency was measured by an encoder. The electric current supplied to the motor was also measured. A box made of the acrylic covered the equipment and was used to prevent some debris from being scattered. A wheeled mobile robot shown in Fig. 20 carried the experimental samples on the plate to the rotor that was fixed on the base.
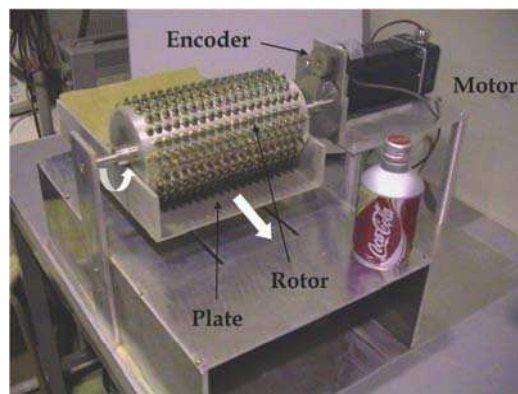

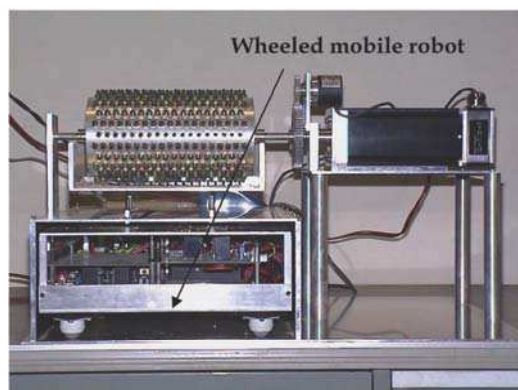Fig. 19. Test equipment for crush (top view).

Fig. 20. Test equipment for crush (side view).

As the experiment samples, we used clods of the loam layer, in which there is nothing explodable. The amount of the clods for one experiment was 160 g. It is true that the samples were more easily broken than the real earth but they were enough to examine the phenomena. The electric current and particle sizes of the samples after the crush were measured according to various conditions: the rotational frequency of the rotor, the length of the bits, the gap between the tip of the bits and the plate fixed under the rotor, and the traveling speed of the robot. They were varied on condition that each standard value was 2100 rpm, 5 mm, 2 mm and 10 mm/s respectively. The particle sizes of the samples after the crush were sorted out at four groups: 0-3 mm, 3-7 mm, 7-10 mm, and over 10 mm. The lengths of 3 mm, 7 mm and 10 mm correspond to the hole size of the square lattice plates used for sorting.
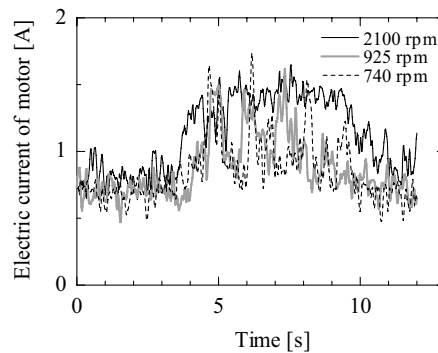
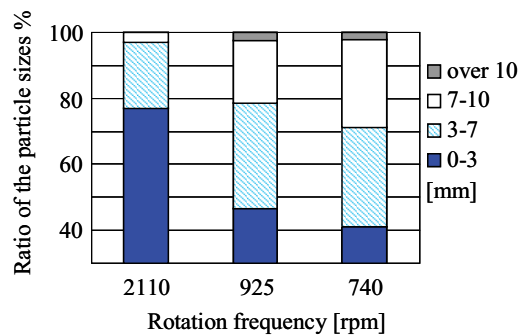Fig. 21. Comparison for the rotational frequencies.

Fig. 22. Comparison for the rotational frequencies.

Figures 21 and 22 show the experimental results to each rotational frequency of the rotor: 2100 rpm, 925 rpm and 740 rpm, which was changed by speed reducers. The voltage supplied to the rotor motor was constant. In the conventional demining machines, the frequency is at most as 700 rpm (Geneva International Centre for Humanitarian Demining, 2002). Figure 21 shows that high rotational frequency leads to continuous crush. Figure 22 shows that high rotational frequency is related to fineness of the particle sizes of the samples after the crush, that is, high processing reliability.
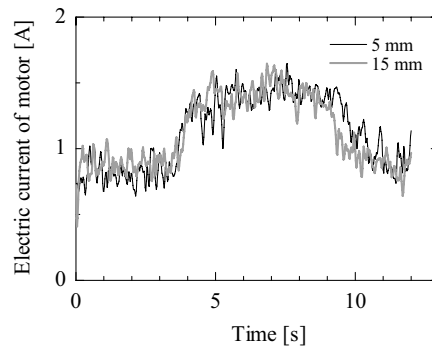
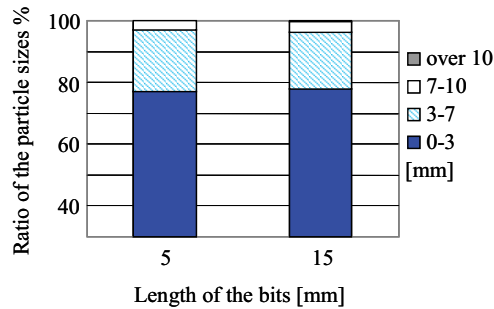Fig. 23. Comparison for the lengths of the bits.

Fig. 24. Comparison for the lengths of the bits.

Figures 23 and 24 show the experimental results to the length of the bits. Each length of the bits was 5 mm and 15 mm except for the length of the mounting parts that was about 5 mm. Both results were almost equal because of the high rotational frequency of the rotor. In case of 15 mm bits, however, there were some debris that passed through the 10 mm square lattice. While, in case of 5 mm bits, no such debris were left.
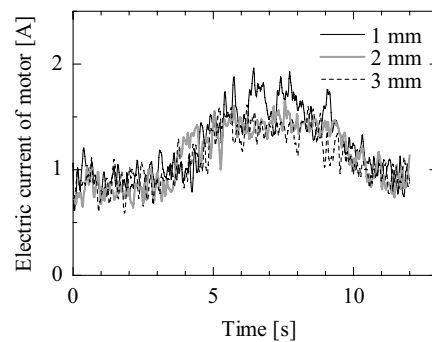
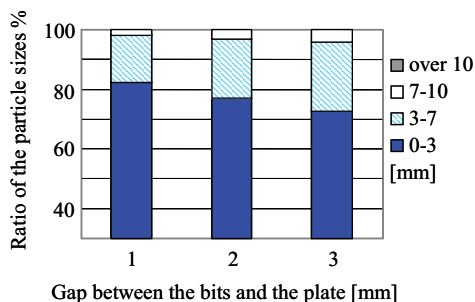Fig. 25. Comparison for the gaps.

Fig. 26. Comparison for the gaps.

Figures 25 and 26 show the experimental results to the gap between the tip of the bits and the plate fixed under the rotor. Three kinds of gaps were examined: 1 mm, 2 mm and 3 mm. The smaller the gap became, the smaller the samples were crushed and the electric current of the motor slightly increased. Therefore, it was confirmed that small distance is desirable for humanitarian demining operation.
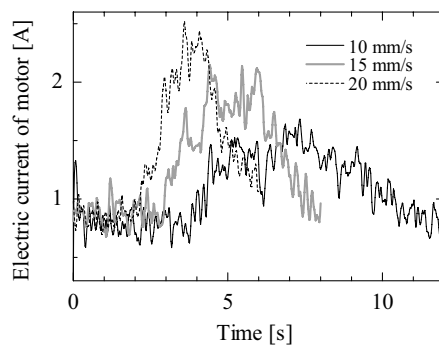

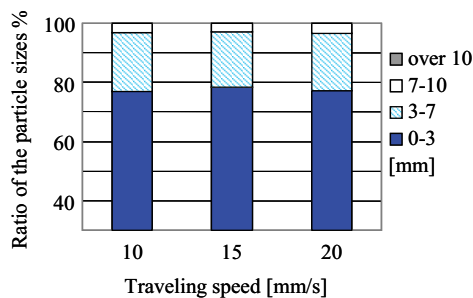Fig. 27. Comparison for the traveling speeds.

Fig. 28. Comparison for the traveling speeds.

Figures 27 and 28 show the experimental results to the three kinds of traveling speeds of the robot: 10 mm/s, 15 mm/s and 20 mm/s. As the robot traveled faster, the maximum value of the electric current of the motor increased. However, there is little difference to the particle

sizes of the samples after the crush. Therefore, in respect of time efficiency, it is desirable that the robot travels fast within the limits of keeping the rotational frequency of the rotor.

7. Summary and Future Works

In this study, we proposed a novel excavation-type demining robot that worked autonomously. The advantages of the robot are a high clearance capability and high efficiency. The crusher inside of the robot plays two roles: crushing the mines and sifting soil. Therefore, the robot has a high clearance capability. It also has a mechanism for separating metal splinters of mines inside. In addition, the robot can perform a series of those operations continuously. So it has high efficiency.

However, this robot is not all-powerful for all environments. The main target area for our robot is the place that becomes the farmland after demining. For example, the areas are plains or past farmland. The reason why we choose farmland as the demining area is that farmland is such an area where local people cannot help entering to live, and so it should be given the highest priority. For severe conditions, it will be necessary to cooperate with other types of machines, robots and some sensors systems.

The kinematics and motion planning for the robot were discussed. The possibility of demining was verified by a scale model of the robot. It was confirmed that 40 cm was the proper depth of excavation through experiments. The crush process that had high reliability was also discussed.

The implementation of a prototype is as follows: the power source for the robot is hydraulic, the required minimum shielding is 10 mm steel plate, and the approximate size and weight are 3.6 $\times$ 8.4 $\times$ 3.0 m in height and 50 t respectively. We assume that the maximum crushable rock size is about 20 $\times$ 20 $\times$ 20 cm. If a bigger and sturdy rock comes into the bucket, the rotor may stop. In this case, the robot will have to stop the operation and to remove the rock. This is our future work. For the navigation system, we use some sensors as follows: the global position of the robot is measured with RTK-GPS. The tilt angles of the body (roll and pitch angles) are measured with clinometers. The orientation angle of the body (yaw angle) is measured with a gyroscope. Stereo video cameras are necessary to measure the corrugation of the ground and to monitor the ground. Laser range finders and ultrasonic sensors are necessary to find the obstacles.

It will need a lot of money to develop and maintain the robot. However, we are convinced that our robot is one of the best solutions concerning a clearance capacity and efficiency. We wish the robot would be provided by an advanced nation as a part of a national contribution.

8. Acknowledgments

9. References

Shimoi, N. (2002). *technology for detecting and clearing LANDMINES*. Morikita Shuppan Co., Ltd., ISBN: 4627945515, (in Japanese).

Geneva International Centre for Humanitarian Demining. (2002). *Mechanical Demining Equipment Catalogue*.

Shibata, T. (2001). Research and Development of Humanitarian Demining in Robotics, *Journal of the Robotics Society of Japan*, 19(6), pp. 689-695, (in Japanese).

Kama, T.; Kato, K. & Hirose, S. (2000). Study of Probe-type Mine Detecting Sensor (Design and Experiments for the Impulsive Probing). *Proceedings of JSME ROBOMEC'00*, pp. 1P1-69-108 (1)-(2), (in Japanese).

Hirose, S. & Kato, K. (2001a). Development of the quadruped walking robot, TITAN-IX - mechanical design concept and application for the humanitarian de-mining robot. *Advanced Robotics*, pp. 191-204.

Hirose, S.; Fukushima, E. F. & Kato, K. (2001b). Automation Technology for Humanitarian Demining Task. *Journal of the Robotics Society of Japan*, 19(6), pp. 722-727, (in Japanese).

Furihata, N. & Hirose, S. (2004). Development of Mechanical Master-Slave Hand for Demining Operation. *Proceedings of International Conference on IEEE Robotics and Automation*, pp. 2017-2024.

Tojo, Y.; Debenest, P.; Fukushima, E. F. & Hirose, S. (2004). Robotic System for Humanitarian Demining. *Proceedings of International Conference on IEEE Robotics and Automation*, pp. 2025-2030.

Shiraishi, Y. & Nonami, K. (2002). Development of Mine Detection Six-Legged Walking Robot COMET-III with Hydraulic Driving System. *Proceedings of 20th Annual Conf. of the Robotics Society of Japan*, 2J15, (in Japanese).

Ushijima, K. (2001). Mine Detection System Using Blimps. *Workshop on Humanitarian Demining of Anti-Personnel Mines*, pp. 55-60, (in Japanese).

Mori, Y.; Takayama, K. & Nakamura, T. (2003). Conceptual Design of an Excavation-type Demining Robot. *Proceedings of the 11th Int. Conf. on Advanced Robotics*, Vol.1, pp. 532-537.

Mori, Y.; Takayama, K.; Adachi, T.; Omote, S. & Nakamura, T. (2005). Feasibility Study on an Excavation-Type Demining Robot. *Autonomous Robots 18, pp. 263-274.*

Jimbo, T. (1997). *Landmine Report (written in Japanese: original title is JIRAI REPORT).* TSUKIJI SHOKAN Co., Ltd., ISBN: 4806768057 , Nov. 1997, (in Japanese).

Mobile Robots: towards New Applications

Edited by Aleksandar Lazinica

The range of potential applications for mobile robots is enormous. It includes agricultural robotics applications, routine material transport in factories, warehouses, office buildings and hospitals, indoor and outdoor security patrols, inventory verification, hazardous material handling, hazardous site cleanup, underwater applications, and numerous military applications. This book is the result of inspirations and contributions from many researchers worldwide. It presents a collection of wide range research results of robotics scientific community. Various aspects of current research in new robotics research areas and disciplines are explored and discussed. It is divided in three main parts covering different research areas: Humanoid Robots, Human-Robot Interaction, and Special Applications. We hope that you will find a lot of useful information in this book, which will help you in performing your research or fire your interests to start performing research in some of the cutting edge research fields mentioned in the book.

How to reference

In order to correctly reference this scholarly work, feel free to copy and paste the following:

Yoshikazu Mori (2006). Feasibility Study on an Excavation-Type Demining Robot PEACE, Mobile Robots: towards New Applications, Aleksandar Lazinica (Ed.), ISBN: 978-3-86611-314-5, InTech, Available from: http://www.intechopen.com/books/mobile_robots_towards_new_applications/feasibility_study_on_an_excavation-type_demining_robot_peace

INTECH
open science | open minds